FAST TRANSVERSE PHASE SPACE MEASUREMENT SYSTEM FOR GUNLAB – A COMPACT TEST FACILITY FOR SRF PHOTOINJECTORS

J. Völker*, T. Kamps, HZB, Berlin, Germany

Abstract

Superconducting radiofrequency photo electron injectors (SRF guns) are promising electron sources for the next generation of electron linear accelerators. The energy recovery linac (ERL) bERLinPro will employ a 1.5 cell 1.3 GHz SRF gun cavity with normal conducting high quantum efficiency photocathode to produce a 100mA CW electron beam with high brightness. We are currently working on a compact test beamline (GunLab) to investigate the phase space of the extracted electron beam and to optimize the drive laser as well RF parameters. The motivation for GunLab is to decouple the SRF gun development from the ERL development. The goal is to measure not only the complete 6 dimensional phase space of the extracted and accelerated bunches but also to investigate dark current and beam halo. In this paper we will discuss unique features of GunLab for the phase space measurements.

MOTIVATION

GunLab is an independent and optimized beamline to characterize electron guns and to investigate different phase space measurement systems for space charge dominated electron bunches at low energies up to 3.5 MeV. A schematic overview is shown in Fig. 1.

A pulsed drive laser extracts electron bunches from a normal conducting photocathode inside a superconducting RF cavity (SRF gun) which accelerates them up to 3.5MeV. A superconducting solenoid will be used to focus the divergent beam and for emittance compensation at a reference point. To investigate the phase space of the bunches as a function of SRF gun and drive laser settings and solenoid focusing strength we want to use a fast phase space measurement system. The longitudinal phase space will be measured by a combination of transverse deflecting cavity (TCAV) [1] and spectrometer dipole [2]. For measurements of the transverse phase space we want to use a combination of two opposite directed steerer magnets (the scanner magnet) and a slit mask. The scanner magnet moves the beam parallel to the beam axis over the slit.

In this paper specification and realization of the scanner system is discussed.

Parameters of GunLab

The expected beam parameters are determined by the injector setup.

A detailed report about the estimated beam parameter as a function of the injector parameters you can find here [3]. Table1 shows the range of the estimated beam parameter.

* jens.voelker@helmholtz-berlin.de

Table 1: SRF Gun Setup and Expected Beam Parameters

Parameter	Value
Drive laser pulse length	3...16 ps (FWHM)
Transversal laser shape	FlatTop
Drive laser repetition rate	1.3 GHz
Macro pulse repetition rate	10 Hz
SRF gun frequency	1.3 GHz
Electric peak field	30 MV/m
Bunch exit energy	1 . . . 3 MeV
Rel. energy spread	0.2%...5%
Bunch charge	0 . . . 100 pC
Bunch length	2...10 ps (rms)
Max. Average current	4 μA
Normalized emittance	0.4...10 mm mrad

TRANSVERSE PHASE SPACE MEASUREMENT

We want to observe the projected and the sliced transverse phase space of the electron bunches with dedicated techniques.

Projected Transverse Phase Space

A direct method to investigate the projected transverse phase space is a pepperpot or a slit mask. The slit samples narrow emittance dominated beamlets out of a space charge dominated beam. For a slit scan the scanner-magnet deflects the beam parallel to the beam axis and through a slit which has a stable position in the middle of the beam tube. The achievable frequency of such a measurement is limited by the power supply[1] for the magnets and the measurement system downstream, which can be a second slit-scanner with a Faraday-Cup (electronic measurement) or for small beam currents a view screen (optical measurement). For the optical measurement the CCD is the limiting factor for the measurement frequency.

Sliced Transverse Phase Space

As another technique to reconstruct the transverse phase space we will perform a slice emittance measurement. Therefore a TCAV together with two quadrupole magnets are installed in GunLab. The developed TCAV is an one cell cavity which can deflect the beam in two directions. For the slice emittance measurement the quadrupoles minimize the beam dimension in one direction on a screen downstream the TCAV. In a second step the TCAV streaks

[1] For magnets with low inductivities DC power supplies can achieve a frequency up to 1 kHz.

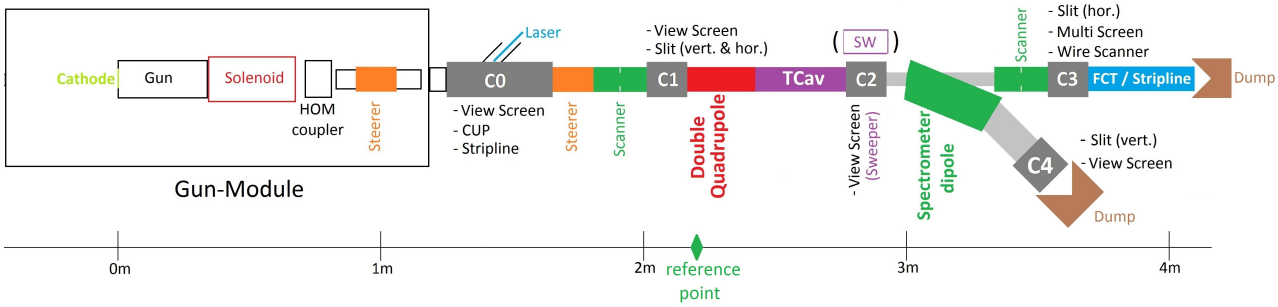

Figure 1: Schematic view of GunLab.

the electron bunch. The resulting image on the screen consist of the temporal distribution in streaked direction and one transverse distribution in the perpendicular direction. The temporal resolution of the slices is a convolution of the beam width in streak direction and the longitudinal profile. The resolution has to be constant for the complete double quadrupole scan. For such a scan the setting of both quadrupole strengths pass a definite function which produce a constant focal length in the streaked direction. Only the beam width in the perpendicular direction changes which will be used to reconstruct the phase space of each slice.

A problem for both methods could be that the used dipole and quadrupole magnets can have a significant impact on the linearity of phase space by non-perfect magnetic fields. The remanent magnetic field is an additionally problem in case of magnets with a yoke. These fields can kick and distort the beam also when the magnet is switched off. A solution are coil dominated magnets for example cos(nθ)-coils. They work without yoke and can produce magnetic fields with suppressed higher magnetic field orders (Sextupole, Dekapole, etc). Therefore cos(θ)-coils as scanner magnets and cos(2θ)-coils as quadrupole magnets are the most promising method for fast projected and sliced emittance measurements without negative influence of the electron phase space.

SHORT COIL DOMINATED MAGNETS

Coil dominated magnets consist of non magnetic materials, hence only the current distribution defines the magnetic field, which can be described as a sum of magnetic multipoles. One example for a coil dominated magnets are the so called cos($n\theta$)-magnets. In theory they produce perfect magnetic n-poles by an azimuthal current distribution around an infinity long round tube which follows a cos(nθ)-function. All but the amplitude of the n-th multi-pole are suppressed. For designing a real magnet one is limited by the dimensions of the cables and it is only possible to approximate these functions. Thereby the resulting magnetic field is not this perfect n-multi-pole any more. Furthermore the used cables need a connection to each other (end caps). The shape of these end caps and the azimuthal distribution of the cables have to be optimized to get a coil designs which produce dipole or quadrupole fields and suppress other multi-poles.This is only possible with the direct calculation of the three dimensional field of the complete magnet.

Field Calculation

The three dimensional magnet field of a coil was calculated by the Biot-Savart law. Therefore the coil was divided into N wires with m_i elements. These elements are straight short line segments with a current I which produce a magnetic field at the position $\vec{P}$. If we neglect material effects the magnetic field could be calculate by [4]:

$$\vec{B}(\vec{P}) = \frac{\mu_0 I}{4\pi} \frac{|\vec{r}_1| + |\vec{r}_2|}{|\vec{r}_1||\vec{r}_2| + \vec{r}_1\vec{r}_2} \frac{\vec{r}_1 \times \vec{r}_1}{|\vec{r}_1||\vec{r}_2|}$$

with $\vec{r}_1$ and $\vec{r}_2$ as the start and end points of the line segment relative to the point $\vec{P}$. These formula can be easily implemented and parallelized in a numerical program like MATLAB.[2]

Geometry of the Line Segments

The next step is the calculation of the positions of each wire of the coil especially for the coil end cap. The main elements of the coil are the wires along the beam pipe which are positioned on a cylinder with the radius R_0 at angle positions θ. For the calculation of the coil end caps we can imagine, that the wires are positioned on the two dimensional surface of the beam pipe. There the wire should follow an elliptical shape with a and b as the principal axes:

$$\begin{aligned} \vec{R}_{2d} &= (a\cos(\phi)\ ,\ b\sin(\phi)) \\ \Rightarrow \vec{R}_{3d} &= \left(R_0 \cos(\frac{R^{(1)}_{2d}}{R_0})\ ,\ R_0 \sin(\frac{R^{(1)}_{2d}}{R_0})\ ,\ R^{(2)}_{2d} \right) \end{aligned}$$

The parameter a can be substituted with the azimuth angle times the beam pipe radius $a = R_0\alpha = R_0(\frac{\pi}{2} - \theta)$.

The next step of the coil design is the transformation of this 2d geometry on the surface of the beam pipe to a real thick magnet coil.

Realization with Copper Foils

The construction should consist of copper foils instead of thick wires. Because with this foils we need only a small

[2] The final code was tested with models which can be calculated analytically.

number of windings and we achieve a more compact wire package as with round wires. The foil will be spooled on an aluminum yoke with the negative contour of the innner coil part. The spin-off of foils is the more complex design of the end caps. Each wire has to be skewed to follow the defined path on the beam tupe. You can see an example of this effect in Fig. 2. It shows the position and rotation of one thin copper foil on the tube. This rotation angle β on top of the tube is given by the binormal unit vector of the function $\vec{R}_{3d}$ and can be calculated in our case to

$$\tan(\beta) = \frac{b}{R_0 \alpha^2}$$

This angle and his dependency of the parameter α and b which differ for each foil winding in one coil has to consider for the numerical design. For a more detailed overview about the geometry of the end caps see [4].

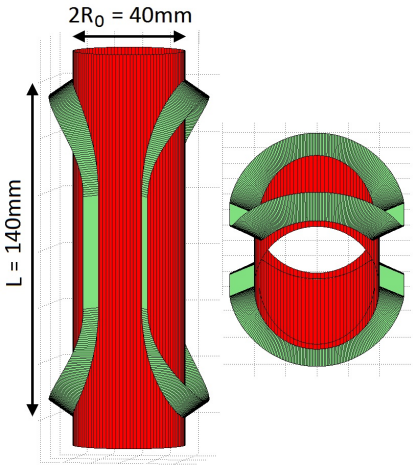

Figure 2: Example for the winding of one wire for Scanner coil (green) on the beam pipe (red).

DESIGN OF THE COSθ-COILS

We apply a numerical minimization of the unwanted beam effects to find the best parameter values for the distribution angle θ, the end cap radius b and the coil thickness d.[3] It is not possible to observe the effects of the magnets by a longitudinal integration of the resulting fields. Therefore the calculated 3d field of the scanner coils or the quadrupoles was implemented as 3d-fields in the tracking code ASTRA [5]. These method shows the real impact on the phase space of the electrons by the magnetic fields. The calculated dipole fields were implemented as a complete Scanner magnet which consist of two dipole coils with the same distance as in the beamline at GunLab (150 mm). For each magnet we observed the average error of the phase space for a given initial electron distribution, which is a zero-emittance, zero-space-charge electron distribution with a rectangle shape in the transverse plane. The average error is than the normalized χ^2-value which is defined as $\chi^2 = \Sigma_i^N (x_i^{(f)} - x_i^{(i)})^2/N$ with the particle number N and the initial $x_i^{(i)}$ and final $x_i^{(f)}$ positions in the phase space. Fig. 3 show χ^2 as a function of d, b and θ_0 for a steerer magnet with a length of 140 mm. Table 2 show the parameter of the dipole and quadrupole magnets which have the minimal effects on the beam.

[3] In normal cases L could be also an independent parameter for the optimization, but for GunLab the overall Length for the magnets is limited which means that L depends on the other 3 parameters.

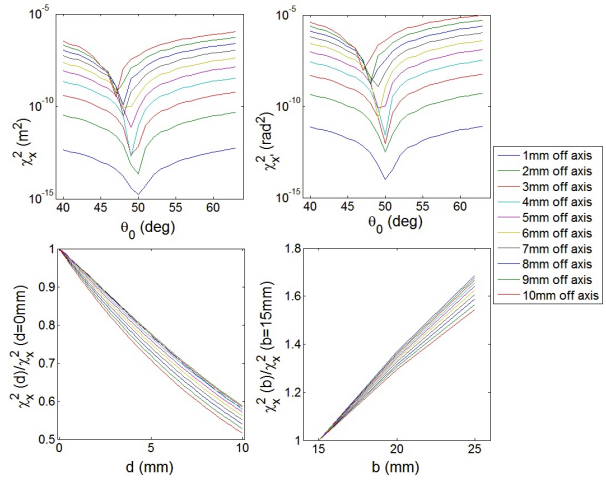

Figure 3: χ^2-values vs Parameter of the Scanner coil.

Table 2: Parameter for the Optimal Coil Dominated Magnets for GunLab

Parameter	**cosθ**	**cos2θ**
θ_{int}	96°	74°
R_0	15 mm	10 mm
d	> 8 mm	> 20 mm
L_{coil}	140 mm	80 mm

EMITTANCE MEASUREMENT WITH THE SLIT-SCANNER

The final scanner coils will be placed in GunLab in front of the slit. Both coils are separated longitudinal with 150 mm (peak to peak) and serially connected (identical absolute magnetic fields but with negative sign). The electron beam enters the first scanner coil centered to the beam pipe and will be deflected by a small angle and re-deflected by the the second scanner so that the beam exits the scanner parallel to the beam pipe axis but off-axis. For a better resolution of the divergence measurement the slit width should be as small as possible, but did not block to much signal. As a good solution it is planed to take a slit width of 100μm. The first tests at GunLab will be done with small average beam currents so that the width of the beamlets has to observed with the optical method. This can be done with luminescent screens in a distance of 700 mm or 1600 mm downstream the slit position. The transverse emittance follows from

the method of second moments with the measured position, beam width and intensity values of the different beamlets.

Transverse Emittance - Method of the Second Moments

The transverse emittance of the electron beam is defined as

$$\varepsilon = \sqrt{< x^2 >< x'^2 > - < xx' >^2}$$

The second moments of the beam ($< x^2 >$,$< x'^2 >$,$< xx' >$) can be calculated by the position ζ_n and the width σ_n of the n-th beamlet on the screen at the distance L behind the slit:

$$\begin{aligned} < x^2 > &= \Sigma_n A_n (x_n - < x >)^2 \\ < x'^2 > &= \Sigma_n A_n (\delta_n^2 + (x'_n - < x' >)^2) \\ < xx' > &= \Sigma_n A_n (x_n x'_n - < x >< x' >) \end{aligned}$$

with the normalization factor A_n, the beam offset x_n at the slit, the divergence $\delta_n = \sigma_n / L$ and the correlated divergence of the beamlet $x'_n = (\zeta_n - x_n)/L$. $< x >= \Sigma_n A_n x_n$ and $< x' >= \Sigma_n A_n x'_n$ are the average values of x_n and x'_n. In case of an optical measurement with a luminescent screen the normalization factor is the ratio of the intensity of the single image to the sum of all images. This method together with the final scanner design was tested by simulations to estimate the uncertainty for the real measurements

Numerical Test of the Emittance Measurement

These simulations consist of tracking electron bunches with 10^5 particles with different transverse emittance and without space charge effects. This simulations was also done with ASTRA. Therefore we define 25 different amplitudes of the magnetic fields in the Scanner coils which deflects horizontally the beam between ≈ -6 and $\approx +6$ mm offset (≈ 0.5 mm step size). At the position of the slit only particle was taken into account which passes the range of the slit width ($\pm 50 \mu$m relative to axis). These particles were tracked a second time through a drift space to the position of the screen. The average position, width and the intensity (number of particles) of the beamlets were used to reconstruct the horizontal emittance of the original bunch. Fig. 4 shows the relative variations of the calculated transverse emittances to theme of the original bunch in front of the slit. The error bars in red and black and the blue line are the numerical and systematic uncertainties of this simulations and the slit scan method with a 100μm slit width. This illustrate that the influence of the magnets to the emittance measurement is not significant to numerical uncertainties, which are less then 1%. More expensive simulations to reduce the numerical error are work in progress.

SUMMARY AND OUTLOOK

A fast transverse phase space measurement system was developed for the new SRF gun test facility at HZB - GunLab. This slit-scanner consist of two cosθ coil magnets which

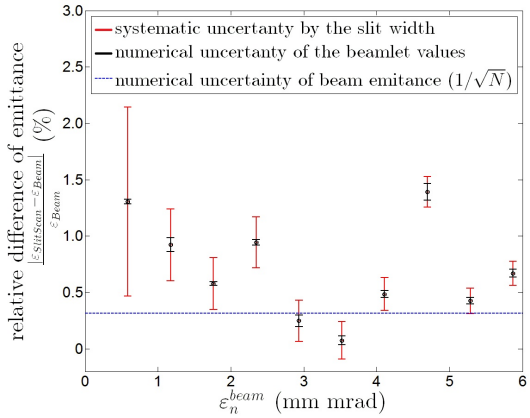

Figure 4: Relative differences between beam emittances and measured emittances by slit scanner.

moves the beam parallel to the beam axis over a slit. We presented the calculation and optimization procedure for the magnets and the influences to the measurements. Furthermore we sketch out that also quadrupole magnets based on the cos(nθ)-coils works and will be used for slice emittance measurements at GunLab. The next steps are the construction, field measurements and tests with beam. This should be done in the next half year so that we can start with beam measurement at GunLab in summer 2015.

REFERENCES

[1] A. Ferrarotto et al.,IPAC'14, June 2014, THPME105.

[2] I.Y.Vladimirov et al., IPAC'14, June 2014, THPME150.

[3] J. Völker et al., IPAC'14, June 2012, MOPRI020.

[4] S. Russenschuck, "Field Computation for Accelerator Magnets", (Weinheim, WILEY-VCH Verlag GmbH & Co., 2010), *ISBN: 978-3-527-40769-9*

[5] K. Floettmann et al., http://www.desy.de/mpyflo/